Scientia Iranica B (2022) 29(3), 1221–1235

Sharif University of Technology
Scientia Iranica
Transactions B: Mechanical Engineering
http://scientiairanica.sharif.edu

Control of active suspension system in the presence of nonlinear spring and damper

S. Kilicaslan*

Department of Mechanical Engineering, Faculty of Engineering, Gazi University, 06570 Maltepe, Ankara, Turkey.

Received 27 April 2021; received in revised form 23 July 2021; accepted 20 September 2021

KEYWORDS
Active suspension system;
Nonlinear spring;
Nonlinear damper;
State-dependent Riccati equation;
Approximating sequence of Riccati equation.

Abstract. The present study developed two simple and easy methods in terms of computation and application using State Dependent Riccati Equation (SDRE) and Approximating Sequence of Riccati Equation (ASRE) techniques to control active suspension system in the presence of nonlinear spring and damper. In addition, this study made a comparison regarding the effectiveness of both control methods developed by the mentioned techniques. To this end, first, the methodologies of both approaches were discussed. Second, the nonlinear dynamics of the vehicle suspension system was described in terms of conveniently selected state variables for better control performance. Third, a cost function was proposed considering the suspension and tire deflections, sprung mass velocity and acceleration, and unsprung mass velocity variables to improve the ride quality, suspension deflection, and tire deflection. In addition, a convenient representation of this cost function in terms of state variables was obtained to realize better control. Two forms of road disturbance were also taken into account called the bump, expressed as a sinusoidal function, and road roughness, expressed as a white noise. Finally, a quarter-car suspension system, which was the equivalent model of Ford Fiesta Mk2, was used as an example to perform simulations using the developed control methods the results of which were compared with the performance requirements and corresponding passive suspension system.

1. Introduction

A number of studies have been conducted on different aspects of suspension systems [1–6]. The growing demands for passengers' ride comfort, handling quality of vehicles, and holding quality of roads have encouraged the application of Active Suspension Systems (ASSs). In the following, a brief review of the conducted studies on ASSs control in the presence of nonlinear springs and dampers is given.

*. *Tel.: +90 312 582 3408; Fax: +90 312 231 9810*
E-mail address: skilicaslan@gazi.edu.tr

doi: 10.24200/sci.2021.58189.5607

Malekshahi et al. [7] designed a predictive multi-input multi-output nonlinear control through an optimization process. The response was predicted using truncated Taylor series expansion. Liang et al. [8] presented an optimal control method. Abdalla et al. [9] employed a linear matrix inequality-based controller.

Pusadkar et al. [10] evaluated a technique using disturbance observer and sliding mode control. Deshpande et al. [11] applied a sliding mode control method with a disturbance observer. Wang et al. [12] used a robust predictive sliding mode control approach in their study. Rath et al. [13] developed an adaptive higher-order sliding mode control law using modified supertwisting and adaptive supertwisting approaches. Wang et al. [14] proposed a control algorithm by combining active disturbance rejection control with fuzzy sliding-mode control. Rui [15] employed the nonlinear adaptive sliding-mode control technique to electronically control air suspension.

Zhang et al. [16] designed a neural network control technique. Huang et al. [17] presented adaptive control and neural network designs. Zhu and Zhu [18] used an adaptive neural network controller.

Pan et al. [19] employed an adaptive control method in their study. Pang et al. [20] applied an adaptive backstepping control technique. Na et al. [21] developed an adaptive control approach. Yao et al. [22] proposed a variable adaptive law control method. Yao et al. [23] designed an adaptive control technique. Qin et al. [24] utilized an adaptive robust control approach. Qin et al. [25] presented an adaptive robust control method considering sky hook model as a servo constraint. Pan et al. [26] considered the robust adaptive control design.

Zhang et al. [27] used an adaptive control method as well as a hysteretic leaf spring in a suspension system. Ding et al. [28] carried out a study based on robust event-triggered control law. Hysteretic leaf spring is also considered in this study.

Wu et al. [29] developed a fault-tolerant control method. Lu et al. [30] proposed the active disturbance rejection control technique. Nourisola and Ahmadi [31] designed H-infinity controller using the genetic algorithm.

Zhang and Jing [32] introduced a switching logic-based saturated control approach. Demir et al. [33] investigated a hybrid fuzzy logic method using fuzzy logic and proportional integral derivative control laws. Aldair and Wang [34] designed an artificial intelligent neuro-fuzzy controller by combining neural network with fuzzy logic methods.

Given that the application of the nonlinear control methods in the previous studies was proven computationally intensive, the present study primarily aimed to propose computationally simple methods for better control of suspension systems with nonlinear springs and dampers. To this end, two methods were developed using State-Dependent Riccati Equation (SDRE) and Approximating Sequence of Riccati Equation (ASRE) to control the nonlinear suspension systems. The proposed methods were computationally simple and easy to apply. In addition, this study made a comparison between the performances of these control methods developed through the mentioned techniques.

SDRE approach has recently drawn considerable attention owing to its advantages such as its simple computation, design flexibility, and applicability in real time. In this approach, nonlinear dynamics is expressed through a State-Dependent Coefficient (SDC) and represented in a linear manner. Given that nonlinear equations are represented by linear equations, the linear control techniques can be used. As a result, this method is an appropriate candidate for designing filter, observer, and controller. Cimen [35] has recently published a complete literature review on the theory of SDRE control. This method has been successfully applied in different areas with nonlinear dynamics including helicopter, spacecraft, satellite, missile, ship, and robot [36].

Another simple method called ASRE was established for systems with nonlinear dynamics. In this method, the nonlinear system is represented through recursive Linear Time Varying (LTV) equations [37]. As mentioned earlier, since the nonlinear equations are represented by linear equations, the linear control methods can be employed. This technique can be used for systems with nonlinear dynamics that satisfy local Lipschitz requirement, which is very mild. This requirement is standard for solution uniqueness. This method was successfully applied to systems with nonlinear dynamics such as helicopter, spacecraft, satellite, missile, ship, and robot, to name a few [38].

The current study investigated the control of ASS in the presence of nonlinear spring and damper. In this regard, two control methods that were computationally simple and easy to apply were developed through the SDRE and ASRE techniques. In addition, the effectiveness of both control methods was evaluated. To this end, first, the required methodologies for both approaches were introduced. Second, the nonlinear dynamics of Suspension System (SS) of the vehicle was elaborated through the first-order differential equations, considering the conveniently selected state variables for better control performance. Third, a cost function was proposed based on suspension and tire deflections, sprung mass velocity and acceleration, and unsprung mass velocity variables to improve the ride quality, suspension deflection, and tire deflection. In addition, a convenient representation of this cost function in terms of state variables was obtained to realize better control. The road disturbances in this study were presented in two forms which were a bump expressed as sinusoidal function and road roughness expressed as white noise. Fourth, by using the variables of states and Riccati differential equation, control input is formed. Finally, the equivalent model of a quarter vehicle SS of Ford Fiesta Mk2 was considered as the example in this study. To evaluate the efficiency of both control methods, simulations were performed using the developed control methods, the performance of which was compared with the performance requirements and that of Passive Suspension System (PSS).

2. SDRE control of nonlinear systems

The demands for SDRE technique applications in designing nonlinear filter, observer, and controller are ever-increasing owing to its several advantages such as design flexibility, simple computation, and real-time application. The nonlinear dynamics in this approach is expressed by SDC and represented by linear like equations. Since the nonlinear equations are represented by linear equations, the linear control techniques can be employed. A nonlinear system can be described by:

$$\dot{\mathbf{y}}(t) = \mathbf{f}(\mathbf{y}) + \mathbf{B}(\mathbf{y})\mathbf{u}(t),$$
$$\mathbf{y}(t_0) = \mathbf{y}_0 \in \Re^n, \tag{1}$$

where $\mathbf{y}(t) \in \Re^n$ is the vector of states, $\mathbf{u}(t) \in \Re^m$ denotes the vector of inputs, and $\mathbf{f}(\mathbf{y}) \in \Re^n$ and $\mathbf{B}(\mathbf{y}) \in \Re^{n\times m}$ are the nonlinear functions.

Assumption 1. The equilibrium point of the system is at the origin $\mathbf{y} = \mathbf{0}$ when $\mathbf{u} = \mathbf{0}$, indicating that $\mathbf{f}(\mathbf{0}) = \mathbf{0}$, $\mathbf{B}(\mathbf{y}) \neq \mathbf{0}\ \forall\ \mathbf{y}$, and $\mathbf{f}(\mathbf{y})$ is a one-time continuously differentiable function of $\mathbf{y}$.

Proposition 1. Under the above assumptions, the mathematical factorization of $\mathbf{f}(\mathbf{y})$ in the form of the state-dependent coefficient $\mathbf{A}(\mathbf{y})\mathbf{y}(t)$ always exist. The related parametrization is expressed by [35]:

$$\mathbf{A}(\mathbf{y}) = \int_0^1 \left.\frac{\partial \mathbf{f}}{\partial \mathbf{y}}\right|_{y=\lambda y} d\lambda, \tag{2}$$

where λ is the dummy variable of integration.

The nonlinear differential equation (Eq. (1)) may be rearranged in a pseudo-linear representation in the form of SDC with a linear structure, as shown below:

$$\dot{\mathbf{y}}(t) = \mathbf{A}(\mathbf{y})\mathbf{y}(t) + \mathbf{B}(\mathbf{y})\mathbf{u}(t),$$
$$\mathbf{y}(t_0) = \mathbf{y}_0 \in \Re^n, \tag{3}$$

where $\mathbf{A}(y) \in \Re^{n\times n}$, and $\mathbf{A}(\mathbf{y})$ and $\mathbf{B}(\mathbf{y})$ are the SDC matrices. Here, linear control techniques can be used because the above differential equation can be considered as a pointwise Linear Time Invariant (LTI) system.

Remark 1. SDC matrix $\mathbf{A}(\mathbf{y})$ is not unique and can be written infinitely many different forms. Therefore, different $\mathbf{A}(\mathbf{y})$ matrices can be used as the design flexibility to improve the performance of the system.

The infinite horizon nonlinear regulator that minimizes the following cost function is taken into account:

$$\mathbf{J} = \frac{1}{2}\mathbf{y}^T(t_f)\mathbf{F}(\mathbf{y}(t_f))\mathbf{y}(t_f) + \frac{1}{2}\int_{t_0}^{t_f} \left\{\mathbf{y}^T(t)\mathbf{Q}(\mathbf{y})\mathbf{y}(t) + \mathbf{u}^T(t)\mathbf{P}(\mathbf{y})\mathbf{u}(t)\right\} dt, \tag{4}$$

where $\mathbf{Q}(\mathbf{y}) \in \Re^{n\times n}$ is the state weighting matrix, $\mathbf{P}(\mathbf{y}) \in \Re^{m\times m}$ the control weighting matrix, $\mathbf{F}(\mathbf{y}(t_f)) \in \Re^{n\times n}$ the endpoint matrix taken as zero in this case, $t_0 = 0$ and $t_f = \infty$.

Condition 1. The weighting parameters satisfy $\mathbf{Q}(\mathbf{y}) = \mathbf{Q^T}(\mathbf{y}) \geq \mathbf{0}$ and $\mathbf{P}(\mathbf{y}) = \mathbf{P}^T(\mathbf{y}) > \mathbf{0}\ \forall\ \mathbf{y}$.

Definition 1. If $\{\mathbf{A}(\mathbf{y}), \mathbf{B}(\mathbf{y})\}$ is pointwise stabilizable (controllable), the SDC representation of the nonlinear system is stabilizable (controllable) [39].

Definition 2. If $\{\mathbf{C}(\mathbf{y}), \mathbf{A}(\mathbf{y})\}$ is pointwise detectable (observable), the SDC representation of the nonlinear system is detectable (observable). Here, $\mathbf{Q}(\mathbf{y}) = \mathbf{C^T}(\mathbf{y})\mathbf{C}(\mathbf{y})$ [39].

Remark 2. The stabilizability condition is satisfied $\forall\ \mathbf{y}$ providing full rank for the $n \times nm$ state-dependent controllability matrix, i.e. Eq. (5), shown in Box I, should be satisfied. The detectability condition is satisfied $\forall\ \mathbf{y}$ providing full rank for the $n \times n^2$ state-dependent observability matrix, i.e., Eq. (6), shown in Box II, should be satisfied. If $\mathbf{Q}(\mathbf{y})$ is selected as $\mathbf{Q}(\mathbf{y}) = \mathbf{Q}^T(\mathbf{y}) > 0$, the detectability condition is satisfied $\forall\ \mathbf{y}$.

Definition 3. If $\mathrm{Re}[\lambda_i(\mathbf{A}(\mathbf{y}))] < \mathbf{0}\ \forall\ \mathbf{y}$, the SDC representation is pointwise Hurwitz. Here, $\lambda_i(\cdot)$, $i = 1, \cdots, n$, represents the eigenvalues of a matrix.

The nonlinear control can be formed using State-

$$\mathrm{rank} = \left(\left[\mathbf{B}(\mathbf{y}) \quad | \quad \mathbf{A}(\mathbf{y})\mathbf{B}(\mathbf{y}) \quad | \quad \cdots \quad | \quad \mathbf{A}^{n-1}(\mathbf{y})\mathbf{B}(\mathbf{y})\right]\right) = n \qquad \forall\ \mathbf{y}. \tag{5}$$

Box I

$$\mathrm{rank}\left(\left[\mathbf{C}^T(\mathbf{y}) \quad | \quad \mathbf{A}^T(y)\mathbf{C}^T(\mathbf{y}) \quad | \quad \cdots \quad | \quad \left(\mathbf{A}^T(\mathbf{y})\right)^{n-1}\mathbf{C}^T(\mathbf{y})\right]\right) = n \qquad \forall\ \mathbf{y}. \tag{6}$$

Box II

Dependent Coefficients (SDCs), as presented below:

$$\mathbf{u}(t) = -\mathbf{P}^{-1}(\mathbf{y})\mathbf{B}^T(\mathbf{y})\mathbf{R}(\mathbf{y})\mathbf{y}, \tag{7}$$

where $\mathbf{R}(\mathbf{y})$ is obtained through the following algebraic SDRE:

$$\mathbf{R}(\mathbf{y})\mathbf{A}(\mathbf{y}) + \mathbf{A}^T(\mathbf{y})\mathbf{R}(\mathbf{y}) - \mathbf{R}(\mathbf{y})\mathbf{B}(\mathbf{y})\mathbf{P}^{-1}(\mathbf{y})\mathbf{B}^T(\mathbf{y})\mathbf{R}(y) + \mathbf{Q}(\mathbf{y}) = 0, \tag{8}$$

to have $\mathbf{R} \geq \mathbf{0}$.

Remark 3. If the system is scalar, parametrization of the SDCs is unique $\forall\, y \neq 0$ and it can be represented as $f(y)/y$. However, if the system is not scalar, parametrization of the SDCs is infinite.

Proposition 2. If the system is multivariable, for different SDC matrices $\mathbf{A}_1(\mathbf{y})$ and $\mathbf{A}_2(\mathbf{y})$, assume:

$$\mathbf{A}(\mathbf{y},\gamma) = \gamma\mathbf{A}_1(\mathbf{y}) + (1-\gamma)\mathbf{A}_2(y), \tag{9}$$

where $\gamma \in \Re$. $\mathbf{A}(\mathbf{y},\gamma)$ gives an infinite number of SDC matrices for any $\gamma \in \Re$ that corresponds to a hyperplane.

Proof. See [35].

Theorem 1. Assume that the SDC form is selected such that $col\{\mathbf{A}(\mathbf{y})\}$ is in the neighborhood about the origin, $\{\mathbf{A}(\mathbf{y}), \mathbf{B}(\mathbf{y})\}$ is pointwise stabilizable, and $\{\mathbf{C}(\mathbf{y}), \mathbf{A}(\mathbf{y})\}$ is pointwise detectable. Then, SDRE nonlinear control generates a locally asymptotically stable solution.

Proof. See [35].

3. ASRE control of nonlinear systems

A majority of nonlinear approaches need strong requirements and complex numerical methods. ASRE is a simple method for systems having nonlinear dynamics. In this method, the nonlinear system can be represented using recursive LTV equations. As nonlinear equations are represented by linear equations, the linear control methods can be used. This technique can be used for systems having nonlinear dynamics that satisfy local Lipschitz requirement, which is very mild.

A nonlinear system can be described as follows:

$$\dot{\mathbf{y}}(t) = \mathbf{f}(\mathbf{y}) + \mathbf{B}(\mathbf{y})\mathbf{u}(t), \qquad \mathbf{y}(t_0) = \mathbf{y}_0 \in \Re^n. \tag{10}$$

In the above equation, $\mathbf{y}(t) \in \Re^n$ denotes the vector of states, $\mathbf{u}(t) \in \Re^m$ stands for the vector of inputs, and $\mathbf{f}(\mathbf{y}) \in \Re^n$ and $\mathbf{B}(\mathbf{y}) \in \Re^{n\times m}$ denote nonlinear functions.

Assumption 2. Equilibrium point of the system is at the origin $\mathbf{y} = \mathbf{0}$ when $\mathbf{u} = \mathbf{0}$, meaning that $\mathbf{f}(\mathbf{0}) = \mathbf{0}$, $\mathbf{B}(\mathbf{y}) \neq \mathbf{0}\ \forall\ \mathbf{y}$ and $\mathbf{f}(\mathbf{y})$ is a one-time continuously differentiable function of $\mathbf{y}$.

Proposition 3. Under the above assumptions, the mathematical factorization of $\mathbf{f}(\mathbf{y})$ in the form of state dependent coefficient $\mathbf{A}(\mathbf{y})\mathbf{y}(t)$ always exist. The parametrization is expressed by [35]:

$$\mathbf{A}(\mathbf{y}) = \int_0^1 \left.\frac{\partial \mathbf{f}}{\partial \mathbf{y}}\right|_{y=\lambda y} d\lambda, \tag{11}$$

where λ is used as dummy variable for integration.

The nonlinear differential equation (Eq. (10)) may be rearranged in pseudo linear representation in SDC form having linear structure:

$$\dot{\mathbf{y}}(t) = \mathbf{A}(\mathbf{y})\mathbf{y}(t) + \mathbf{B}(\mathbf{y})\mathbf{u}(t), \qquad \mathbf{y}(t_0) = \mathbf{y}_0 \in \Re^n, \tag{12}$$

where $\mathbf{A}(\mathbf{y}) \in \Re^{n\times n}$. $\mathbf{A}(\mathbf{y})$ and $\mathbf{B}(\mathbf{y})$ are called as SDC matrices. Since the above differential equation is in pseudo linear form, linear control techniques can be used.

Remark 4. SDC matrix $\mathbf{A}(\mathbf{y})$ is not unique and it can be written infinitely in many different forms. Therefore different $\mathbf{A}(\mathbf{y})$ can be used as a design flexibility to improve the performance of the system.

Finite horizon nonlinear regulator that minimizes the following cost function is considered:

$$\mathbf{J} = \frac{1}{2}\mathbf{y}^T(t_f)\mathbf{F}(\mathbf{y}(t_f))\mathbf{y}(t_f) + \frac{1}{2}\int_{t_0}^{t_f} \left\{\mathbf{y}^T(t)\mathbf{Q}(\mathbf{y})\mathbf{y}(t) + \mathbf{u}^T(t)\mathbf{P}(\mathbf{y})\mathbf{u}(t)\right\} dt, \tag{13}$$

where $\mathbf{Q}(\mathbf{y}) \in \Re^{n\times n}$ stands for the state weighting matrix, $\mathbf{P}(\mathbf{y}) \in \Re^{m\times m}$ denotes the control weighting matrix, $\mathbf{F}(\mathbf{y}(t_f)) \in \Re^{n\times n}$ stands for the endpoint matrix, $t_0 = 0$, t_f is finite.

Condition 2. Weighting parameters satisfy $\mathbf{Q}(\mathbf{y}) = \mathbf{Q}^T(\mathbf{y}) \geq 0$ and $\mathbf{P}(\mathbf{y}) = \mathbf{P}^T(\mathbf{y}) > 0\ \forall\ \mathbf{y}$.

Remark 5. If the system is scalar, parametrization of the SDCs is unique $\forall\, y \neq 0$ and it can be represented as $f(y)/y$. However, if the system is not scalar, parametrization of the SDC is infinite.

Proposition 4. If the system is multivariable, for different SDC matrices $\mathbf{A}_1(\mathbf{y})$ and $\mathbf{A}_2(\mathbf{y})$, assume that:

$$\mathbf{A}(\mathbf{y},\gamma) = \gamma\mathbf{A}_1(\mathbf{y}) + (1-\gamma)\mathbf{A}_2(\mathbf{y}), \tag{14}$$

where $\gamma \in \Re$. $\mathbf{A}(\mathbf{y},\gamma)$ gives an infinite number of SDC matrices for any $\gamma \in \Re$ which corresponds to a hyperplane.

Proof. See [35].

The minimization of the nonlinear cost function in Eq. (13), subjected to the nonlinear differential equation (Eq. (12)), can be expressed through successive LTV approximations of both Eqs. (12) and (13) [37]:

$$\dot{\mathbf{y}}^{[0]}(t) = \mathbf{A}(\mathbf{y}_0)\mathbf{y}^{[0]}(t) + \mathbf{B}(\mathbf{y}_0)\mathbf{u}^{[0]}(t),$$

$$\mathbf{y}^{[0]}(t) = \mathbf{y}_0, \tag{15}$$

$$\mathbf{J}^{[0]} = \frac{1}{2}\mathbf{y}^{T^{[0]}}(t_f)\mathbf{F}(\mathbf{y}(t_f))\mathbf{y}^{[0]}(t_f) + \frac{1}{2}\int_{t_0}^{t_f}\left\{\mathbf{y}^{T[0]}(t)\mathbf{Q}(\mathbf{y}_0)\mathbf{y}^{[0]}(t) + \mathbf{u}^{T[0]}(t)\mathbf{P}(\mathbf{y}_0)\mathbf{u}^{[0]}(t)\right\} dt. \tag{16}$$

Here, the first approximation is evaluated using the initial values of the state variables resulting LTI system. When the iteration number $k \geq 1$, the following approximations can be written that refer to LTV system:

$$\dot{\mathbf{y}}^{[k]}(t) = \mathbf{A}\left(\mathbf{y}^{[k-1]}(t)\right)\mathbf{y}^{[k]}(t) + \mathbf{B}\left(\mathbf{y}^{[k-1]}(t)\right)\mathbf{u}^{[k]}(t)$$

$$k \geq 1, \qquad \mathbf{y}^{[k]}(0) = \mathbf{y}_0, \tag{17}$$

$$\mathbf{J}^{[k]} = \frac{1}{2}\mathbf{y}^{T[k]}(t_f)\mathbf{F}(\mathbf{y}(t_f))\mathbf{y}^{[k]}(t_f) + \frac{1}{2}\int_{t_0}^{t_f}\left\{\mathbf{y}^{T[k]}(t)\mathbf{Q}\left(\mathbf{y}^{[k-1]}(t)\right)\mathbf{y}^{[k]}(t) + \mathbf{u}^{T[k]}(t)\mathbf{P}\left(\mathbf{y}^{[k-1]}(t)\right)\mathbf{u}^{[k]}(t)\right\} dt, \qquad k \geq 1. \tag{18}$$

The LTV approximation of the optimal control input can be formed as:

$$\mathbf{u}^{[k]}(t) = -\mathbf{P}^{-1}\left(\mathbf{y}^{[k-1]}(t)\right)\mathbf{B}^T\left(\mathbf{y}^{[k-1]}(t)\right)\mathbf{R}^{[k]}(t)\mathbf{y}^{[k]}(t), \tag{19}$$

where $\mathbf{R}^{[k]}(t)$ is obtained from the following algebraic ASRE:

$$\dot{\mathbf{R}}^{[k]}(t) = -\mathbf{A}^T\left(\mathbf{y}^{[k-1]}(t)\right)\mathbf{R}^{[k]}(t) - \mathbf{R}^{[k]}(t)\mathbf{A}\left(\mathbf{y}^{[k-1]}(t)\right) - \mathbf{Q}\left(\mathbf{y}^{[k-1]}(t)\right) - \mathbf{R}^{[k]}(t)\mathbf{B}\left(\mathbf{y}^{[k-1]}(t)\right)\mathbf{P}^{-1}\left(\mathbf{y}^{[k-1]}(t)\right)\mathbf{B}^T\left(\mathbf{y}^{[k-1]}(t)\right)\mathbf{R}^{[k]}(t),$$

$$\mathbf{R}^{[k]}(t_f) = \mathbf{F}(\mathbf{y}(t_f)). \tag{20}$$

Therefore, the LTV approximation of the closed-loop system can be represented as:

$$\dot{\mathbf{y}}^{[0]}(t) = \hat{\mathbf{A}}(\mathbf{y}_0)\mathbf{y}^{[0]}(t), \qquad \mathbf{y}^{[0]}(t) = \mathbf{y}_0, \tag{21}$$

$$\dot{\mathbf{y}}^{[k]}(t) = \hat{\mathbf{A}}\left(\mathbf{y}^{[k-1]}(t)\right)\mathbf{y}^{[k]}(t),$$

$$k \geq 1, \quad \mathbf{y}^{[k]}(0) = \mathbf{y}_0. \tag{22}$$

Here:

$$\hat{\mathbf{A}}\left(\mathbf{y}^{[k-1]}(t)\right) = \mathbf{A}\left(\mathbf{y}^{[k-1]}(t)\right) - \mathbf{B}\left(\mathbf{y}^{[k-1]}(t)\right)\mathbf{P}^{-1}\left(\mathbf{y}^{[k-1]}(t)\right)\mathbf{B}^T\left(\mathbf{y}^{[k-1]}(t)\right)\mathbf{R}^{[k]}. \tag{23}$$

The convergence of LTV system to the original nonlinear system is explained in Theorem 2.

Theorem 2. Assume that the subsequent conditions on $\mathbf{A}(\mathbf{y})$ and $\mathbf{B}(\mathbf{y})$ hold:

$$(1) \quad \mu\mathbf{A}(\mathbf{y}) \leq \mu_0 \qquad \forall\, \mathbf{y} \in \Re^n, \tag{24}$$

$$(2) \quad \|\mathbf{A}(\mathbf{y}) - \mathbf{A}(\mathbf{x})\| \leq \alpha\|\mathbf{y} - \mathbf{x}\| \qquad \forall\, \mathbf{y}, \mathbf{x} \in \Re^n, \tag{25}$$

$$(3) \quad \|\mathbf{B}(\mathbf{y}) - \mathbf{B}(\mathbf{x})\| \leq \beta\|\mathbf{y} - \mathbf{x}\| \qquad \forall\, \mathbf{y}, \mathbf{x} \in \Re^n, \tag{26}$$

$$(4) \quad \|\mathbf{B}(\mathbf{y})\| \leq \gamma \qquad \forall\, \mathbf{y} \in \Re^n, \tag{27}$$

where $\mu\mathbf{A}(\mathbf{y})$ is the logarithmic norm of $\mathbf{A}(\mathbf{y})$, and α, β, and γ are the constants. Then, while minimizing the approximated cost function $\mathbf{J}^{[k]}$, approximations of the states $\mathbf{y}^{[k]}(t)$ and controls $\mathbf{u}^{[k]}(t)$ converge to the nonlinear system states $\mathbf{y}(t)$ and controls $\mathbf{u}(t)$, minimizing nonlinear cost function $\mathbf{J}$.

Proof. Assume that $\mathbf{\Phi}^{[k-1]}(t, t_0)$ denotes the transition matrix of $\mathbf{A}(\mathbf{y}^{[k-1]}(t))$. Therefore, $\mathbf{\Phi}^{[k-1]}(t, t_0)$ follows the subsequent Brauer's inequality:

$$\left\|\mathbf{\Phi}^{[k-1]}(t, t_0)\right\| \leq \exp\left[\int_{t_0}^{t}\mu\mathbf{A}\left(\mathbf{y}^{[k-1]}(\tau)\right)d\tau\right]. \tag{28}$$

Based on Assumptions 1 and 2, we have:

$$\left\|\mathbf{\Phi}^{[k-1]}(t, t_0) - \mathbf{\Phi}^{[k-2]}(t, t_0)\right\| \leq \alpha\exp(\mu(t - t_0))(t - t_0)\sup_{s\in[t_0,t]}\left\|\mathbf{y}^{[k-1]}(s) - \mathbf{y}^{[k-2]}(s)\right\|. \tag{29}$$

Based on the above equation and Assumptions (1)–(4), the following equation can be obtained as:

$$\begin{aligned}\boldsymbol{\zeta}^{[k]}(t) \leq & \alpha t \exp(\mu_0 t)\boldsymbol{\zeta}^{[k-1]}(t)\|\mathbf{y}_0\| \\ & + \int_0^t \exp(\mu_0(t-s))\gamma\boldsymbol{\zeta}^{[k]}(s)ds \\ & + \|\mathbf{y}_0\| \int_0^t \exp(\mu_0(t-s))\beta\boldsymbol{\zeta}^{[k-1]}(s) \\ & \exp((\mu_0+\gamma)s)ds \\ & + \|\mathbf{y}_0\| \int_0^t \alpha(t-s)\exp(\mu_0(t-s))\gamma\boldsymbol{\zeta}^{[k-1]}(t) \\ & \exp((\mu_0+\gamma)s)ds, \end{aligned} \tag{30}$$

where:

$$\boldsymbol{\zeta}^{[k]}(t) = \sup_{t\in[0,t]} \left\|\mathbf{y}^{[k]}(t) - \mathbf{y}^{[k-1]}(t)\right\|. \tag{31}$$

Since:

$$\left\|\mathbf{y}^{[k]}(t)\right\| \leq \exp((\mu_0+\gamma)t)\,\|\mathbf{y}_0\|, \tag{32}$$

then:

$$\boldsymbol{\zeta}^{[k]}(t) \leq \lambda(t)\boldsymbol{\zeta}^{[k-1]}(t). \tag{33}$$

In the above equation:

$$\begin{aligned}\lambda(t) = & \|\mathbf{y}_0\| \left[\alpha t \exp(\mu_0 t) + \left(\frac{\beta}{\gamma}+\alpha\right)(\exp((\mu_0+\gamma)t)\right. \\ & \left. - \exp(\mu_0 t))\right] \Big/ \left[1-\gamma\int_0^t \exp(\mu_0(t-s))ds\right]. \end{aligned} \tag{34}$$

Therefore, if $|\lambda(t)| < 1\ \forall\ t \in [0,T]$, then $\mathbf{y}^{[k]}(t) \to \mathbf{y}(t)$ on $C([t_0,T],\Re^n)$.

4. Dynamic model

Quarter vehicle ASS was taken into account to demonstrate the effectiveness of the control methods in SS. The vertical motion of the quarter vehicle ASS can be represented as a system with two Degrees of Freedom (DOF), as shown in Figure 1.

The mass of the vehicle body is called the sprung mass represented by m_s; and the masses of the tire and axles are referred to as the unsprung mass represented by m_u. The nonlinearity of the SS was modeled by nonlinear spring and nonlinear damper. While k_s and k_{ns} represent the nonlinear spring constants, b_s and b_{ns} denote the nonlinear damper constants. F_a is the magnitude of the driving force. The stiffness of the tire is determined by the spring whose coefficient is k_t. p_s is the position of the sprung mass, p_u the position of the unsprung mass, and p_r the road disturbance at the position level. The forces imposed by the nonlinear spring and nonlinear damper of the SS can be modeled through the following equations [40]:

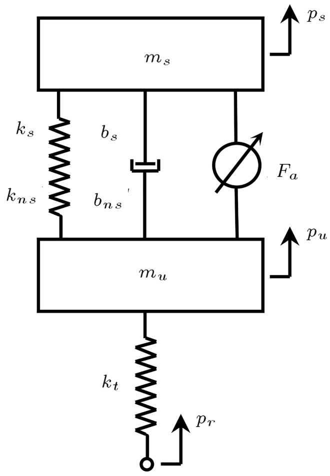

Figure 1. Quarter vehicle ASS.

$$F_s = k_s(p_s - p_u) + k_{ns}(p_s - p_u)^3, \tag{35}$$

$$F_d = b_s(\dot{p}_s - \dot{p}_u) + b_{ns}(\dot{p}_s - \dot{p}_u)^2 \operatorname{sgn}(\dot{p}_s - \dot{p}_u). \tag{36}$$

The dynamic equations of the two-DOF quarter vehicle ASS are obtained as follows:

$$\begin{aligned} m_s\ddot{p}_s & + b_s(\dot{p}_s - \dot{p}_u) + b_{ns}(\dot{p}_s - \dot{p}_u)^2 \operatorname{sgn}(\dot{p}_s - \dot{p}_u) \\ & + k_s(p_s - p_u) + k_{ns}(p_s - p_u)^3 = F_a, \end{aligned} \tag{37}$$

$$\begin{aligned} m_u\ddot{p}_u & - b_s(\dot{p}_s - \dot{p}_u) - b_{ns}(\dot{p}_s - \dot{p}_u)^2 \operatorname{sgn}(\dot{p}_s - \dot{p}_u) \\ & - k_s(p_s - p_u) - k_{ns}(p_s - p_u)^3 + k_t(p_u - p_r) \\ & = -F_a. \end{aligned} \tag{38}$$

Since the selection of state variables plays a key role in better control performance, convenient state variables can be chosen as:

$$y_1 = p_s - p_u, \tag{39}$$

$$y_2 = \dot{p}_s, \tag{40}$$

$$y_3 = p_u - p_r, \tag{41}$$

$$y_4 = \dot{p}_u, \tag{42}$$

where y_1 is the suspension deflection (rattle space), y_2 the sprung mass absolute velocity, y_3 the tire deflection, and y_4 the unsprung mass absolute velocity. As a result, we have the following state equations:

$$\dot{\mathbf{y}}(t) = \mathbf{A}(\mathbf{y})\mathbf{y}(t) + \mathbf{B}u(t) + \mathbf{L}\dot{\mathbf{p}}_r(t). \tag{43}$$

Here, $\mathbf{A}(\mathbf{y})$ is given by Eq. (44) as shown in Box III. $\mathbf{B}$ is given as follows:

$$\mathbf{B} = \begin{bmatrix} 0 & \frac{1}{m_s} & 0 & -\frac{1}{m_u} \end{bmatrix}^T. \tag{45}$$

$\mathbf{L}$ is denoted by:

$$\mathbf{L} = \begin{bmatrix} 0 & 0 & -1 & 0 \end{bmatrix}^T. \tag{46}$$

$\mathbf{y}(t)$ is formed as:

$$\mathbf{y}(t) = \begin{bmatrix} y_1 & y_2 & y_3 & y_4 \end{bmatrix}^T. \tag{47}$$

$u(t)$ takes the following form:

$$u(t) = F_a. \tag{48}$$

Through the following cost function, the suspension and tire deflections, sprung mass velocity and acceleration, and unsprung mass velocity were minimized to improve the ride quality, suspension deflection, and tire deflection.

$$J = \lim_{T \to t_f} \left[\int_0^T \left(\dot{y}_2^2 + \rho_1 y_1^2 + \rho_2 y_2^2 + \rho_3 y_3^2 + \rho_4 y_4^2 \right) dt \right]. \tag{49}$$

To realize better control, a convenient representation of the above cost function in terms of state variables can be obtained as given below:

$$J = \lim_{T \to t_f} \left\{ \int_0^T \left[\mathbf{y}^T(t)\mathbf{Q}(\mathbf{y})\mathbf{y}(t) + 2\mathbf{y}^T(t)\mathbf{N}(y)\mathbf{u}(t) + \mathbf{u}^T(t)Pu(t) \right] dt \right\}. \tag{50}$$

The entries of the symmetric matrix $\mathbf{Q}(\mathbf{y})$ are presented below:

$$Q(1,1) = \frac{k_s^2}{m_s^2} + 2\frac{k_s k_{ns}}{m_s^2} y_1^2 + \frac{k_{ns}^2}{m_s^2} y_1^4 + \rho_1, \tag{51}$$

$$Q(1,2) = \frac{k_s b_s}{m_s^2} + \frac{k_{ns} b_s}{m_s^2} y_1^2 + \left(\frac{k_s b_{ns}}{m_s^2} + \frac{k_{ns} b_{ns}}{m_s^2} y_1^2 \right)(y_2 - y_4)\mathrm{sgn}(y_2 - y_4), \tag{52}$$

$$Q(1,3) = 0, \tag{53}$$

$$Q(1,4) = -\frac{k_s b_s}{m_s^2} - \frac{k_{ns} b_s}{m_s^2} y_1^2 + \left(\frac{k_s b_{ns}}{m_s^2} + \frac{k_{ns} b_{ns}}{m_s^2} y_1^2 \right) y_4 \mathrm{sgn}(y_2 - y_4), \tag{54}$$

$$Q(2,2) = \frac{b_s^2}{m_s^2} + 2\frac{b_s b_{ns}}{m_s^2} y_2 \mathrm{sgn}(y_2 - y_4) + \frac{b_{ns}^2}{m_s^2} y_2^2 [\mathrm{sgn}(y_2 - y_4)]^2 + \rho_2 \tag{55}$$

$$Q(2,3) = 0, \tag{56}$$

$$Q(2,4) = -\frac{b_s^2}{m_s^2} - 3\frac{b_s b_{ns}}{m_s^2}(y_2 - y_4)\mathrm{sgn}(y_2 - y_4) + \frac{b_{ns}^2}{m_s^2}\left(-2y_2^2 + 3y_2 y_4 - 2y_4^2\right)[\mathrm{sgn}(y_2 - y_4)]^2 - \left(\frac{k_s b_{ns}}{m_s^2} + \frac{k_{ns} b_{ns}}{m_s^2} y_1^2 \right) y_1 \mathrm{sgn}(y_2 - y_4), \tag{57}$$

$$Q(3,3) = \rho_3, \tag{58}$$

$$Q(3,4) = 0, \tag{59}$$

$$Q(4,4) = \frac{b_s^2}{m_s^2} - 2\frac{b_s b_{ns}}{m_s^2} y_4 \mathrm{sgn}(y_2 - y_4) + \frac{b_{ns}^2}{m_s^2} y_4^2 [\mathrm{sgn}(y_2 - y_4)]^2 + \rho_4. \tag{60}$$

The entries of $\mathbf{N}(\mathbf{y})$ are as follows:

$$N(1,1) = -\frac{k_s}{m_s^2} - \frac{k_{ns}}{m_s^2} y_1^2, \tag{61}$$

$$N(2,1) = -\frac{b_s}{m_s^2} - \frac{b_{ns}}{m_s^2}(y_2 - y_4)\mathrm{sgn}(y_2 - y_4), \tag{62}$$

$$N(3,1) = 0, \tag{63}$$

$$\mathbf{A}(\mathbf{y}) = \begin{bmatrix} 0 & 1 & 0 & -1 \\ -\frac{k_s}{m_s} - \frac{k_{ns}}{m_s} y_1^2 & -\frac{b_s}{m_s} - \frac{b_{ns}}{m_s}(y_2 - y_4)\mathrm{sgn}(y_2 - y_4) & 0 & \frac{b_s}{m_s} + \frac{b_{ns}}{m_s}(y_2 - y_4)\mathrm{sgn}(y_2 - y_4) \\ 0 & 0 & 0 & 1 \\ \frac{k_s}{m_u} + \frac{k_{ns}}{m_u} y_1^2 & \frac{b_s}{m_u} + \frac{b_{ns}}{m_u}(y_2 - y_4)\mathrm{sgn}(y_2 - y_4) & -\frac{k_t}{m_u} & -\frac{b_s}{m_u} - \frac{b_{ns}}{m_u}(y_2 - y_4)\mathrm{sgn}(y_2 - y_4) \end{bmatrix}. \tag{44}$$

Box III

$$N(4,1) = \frac{b_s}{m_s^2} + \frac{b_{ns}}{m_s^2}(y_2 - y_4)\text{sgn}(y_2 - y_4). \tag{64}$$

Scalar P is given below:

$$P = \frac{1}{m_s^2}. \tag{65}$$

To minimize the cost function (Eq. (50)) imposed to the SS nonlinear differential equation (Eq. (43)), the following nonlinear control law can be formed as:

$$u(t) = -P^{-1}\left[\mathbf{B}^T\mathbf{R}(\mathbf{y}) + \mathbf{N}^T(\mathbf{y})\right]\mathbf{y}(t). \tag{66}$$

Here, $\mathbf{R}(\mathbf{y})$ is given by the following RDE:

$$\begin{aligned}\dot{\mathbf{R}}(\mathbf{y}) = &-\left[\mathbf{A}(\mathbf{y}) - \mathbf{B}P^{-1}\mathbf{N}^T(\mathbf{y})\right]^T\mathbf{R}(\mathbf{y})\\ &-\mathbf{R}(\mathbf{y})\left[\mathbf{A}(\mathbf{y}) - \mathbf{B}P^{-1}\mathbf{N}^T(\mathbf{y})\right]\\ &-\left[\mathbf{Q}(\mathbf{y}) - \mathbf{N}(\mathbf{y})P^{-1}\mathbf{N}^T(\mathbf{y})\right]\\ &+\mathbf{R}(\mathbf{y})\mathbf{B}P^{-1}\mathbf{B}^T\mathbf{R}(\mathbf{y}).\end{aligned} \tag{67}$$

Two different road disturbances were taken into account in this study:

a) Road roughness;

b) Bumps on the road.

Road roughness is taken as a stochastic process represented by a stationary first-order filtered white noise whose Power Spectral Density (PSD) function can be expressed as [41]:

$$\psi(\omega) = \frac{\sigma^2}{\pi}\frac{av}{\omega^2 + a^2v^2}, \tag{68}$$

where v is the speed of the vehicle, ω the circular frequency, σ^2 the variance of road roughness, and a the constant. The values for σ and a were selected based on the type of road roughness. The disturbance $p_r(t)$ caused by the road roughness is expressed through the PSD function in Eq. (68). It was constructed based on a linear filter, whose dynamics are expressed below, and a white noise process [41]:

$$\dot{p}_r(t) = avp_r(t) + w(t), \tag{69}$$

where $w(t)$ denotes a Gaussian white noise process whose intensity is $2\sigma av$. Solution of the above differential equation yields the following equation:

$$p_r(t) = e^{avt}p_r(0) + \int_0^t e^{av(t-\tau)}w(t)d\tau. \tag{70}$$

When the following condition is satisfied:

$$a^2v^2 << \omega^2, \tag{71}$$

then, Eqs. (68) and (69) take the following forms:

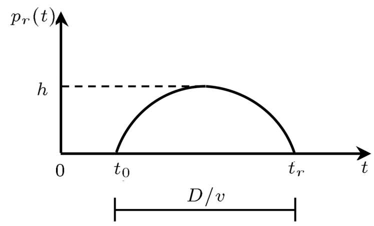

Figure 2. Sinusoidal hump.

$$\psi(\omega) = \frac{\sigma^2}{\pi}\frac{av}{\omega^2}, \tag{72}$$

$$\dot{p}_r(t) = w(t). \tag{73}$$

It refers to the integrated white noise as the road roughness profile. A hump represented by a sinusoidal function is expressed as:

$$p_r(t) = \begin{cases}\frac{h}{2}\left\{1 - \cos\left[\left(\frac{2\pi v}{D}\right)(t - t_0)\right]\right\} & t_0 \le t \le t_r\\ 0 & \text{otherwise}\end{cases} \tag{74}$$

where h denotes the hump height, D the hump width, t_0 the time where the hump starts, and t_r the time where the hump finishes for the tire motion. Therefore, t_r can be represented by sinusoidal hump parameters t_0, D, and v, as demonstrated in the following:

$$t_r = t_0 + \frac{D}{v}. \tag{75}$$

The sinusoidal hump is demonstrated in Figure 2.

5. Case studies

In the present study, the equivalent model of a quarter vehicle SS of Ford Fiesta Mk2 was used as an example, and simulation results of the developed control methods from SDRE and ASRE approaches were checked against the performance requirements and the corresponding PSS in which there is no control to show the effectiveness of both control methods. Moreover, effectiveness of these control methods was compared. The subsequent performance parameters were used to test the effectiveness of each control method [42]:

1. Suspension deflection steady-state error should be kept as closely as possible to zero in the control methods;
2. The maximum value of suspension deflection should be below 0.1 m;
3. The maximum value of the actuator force should be below the static weight of the vehicle;
4. The dynamic tire load should be less than, or equal to, the static weight of the vehicle for good road holding;

5. The maximum value of the sprung mass acceleration should be below 4.5 m/s^2 for good ride comfort [43].

The numerical values of the sprung mass, m_s, and unsprung mass, m_u, in the equivalent quarter vehicle Ford Fiesta Mk2 SS are 216.75 kg and 28.85 kg, respectively. The coefficients of the nonlinear spring between the sprung and unsprung masses, called k_s and k_{ns}, are 21700 N/m and 2170 N/m, respectively. The coefficients of the nonlinear damper between sprung and unsprung masses, i.e., b_s and b_{ns}, are 1200 Ns/m and 120 Ns/m, respectively. Finally, the coefficient of the tire stiffness in the vertical direction, k_t, is 184000 N/m [40].

The values for the following parameters in a sinusoidal hump as a disturbance are as follows: the height of the hump, h, is 0.1 m; the width of the hump, D, is 0.5 m; and the time when the hump starts, t_0, is 0 s.

The road roughness as another disturbance is regarded as a stationary Wiener process whose derivative is considered as a white noise with the intensity of $2\sigma a v$. The values for the parameters a and road roughness variance are 0.15 m^{-1} and 9×10^{-6} m^2, respectively, in the case of asphalt road.

The equilibrium positions of both sprung and unsprung masses were used for measurements. Euler method and MATLAB® were used for numerical integration and simulations, respectively. The sampling time interval in these simulations was 0.001 s. In addition, trial-and-error methods were employed to select the weighting coefficients. After a few trials, the proper weighting coefficients were found as $\rho_1 = 1200$, $\rho_2 = 58$, $\rho_3 = 1200$, and $\rho_4 = 58$. Finally, the endpoint matrix was considered to be as $\mathbf{F} = \mathbf{0}$.

In order to evaluate and compare the performances of both control methods, three different vehicle speeds were taken into account for each of which the performance parameter were fulfilled using both control methods.

The performance parameters of PSS in which there is no control were calculated and compared with those of ASS. In both control methods at each vehicle speed, the suspension deflection steady-state errors were kept close to zero and the maximum values of suspension deflection, tire deflection, and sprung mass acceleration were below 31×10^{-3} m, 5.4×10^{-3} m, and below 4.1 m/s^2, respectively. In addition, under the same condition, the maximum values for the actuator force were below the static weight of the vehicle and those of the dynamic tire loads were below the static weight of the vehicle. Table 1 presents the performance parameters of the SS based on the maximum (peak) and Root Mean Square (RMS) values of the variables at each vehicle speed.

Table 1. Performance parameters of vehicle SS for three different vehicle speeds.

v (m/s)			y_1 (m)	$\dot{y}_2$ (m/s^2)	y_3 (m)	u (N)
10	Active: SDRE	RMS	3.8168×10^{-3}	5.2049×10^{-1}	6.0475×10^{-4}	185.1491
		Peak	30.2672×10^{-3}	40.1542×10^{-1}	53.0111×10^{-4}	1279.2901
	Active: ASRE	RMS	3.8184×10^{-3}	5.1987×10^{-1}	6.0631×10^{-4}	188.4113
		Peak	30.1537×10^{-3}	40.1300×10^{-1}	53.0658×10^{-4}	1351.4710
	Passive	RMS	7.5020×10^{-3}	13.2585×10^{-1}	13.0028×10^{-4}	
		Peak	57.2637×10^{-3}	105.2187×10^{-1}	113.2754×10^{-4}	
20	Active: SDRE	RMS	2.2206×10^{-3}	3.4430×10^{-1}	4.6963×10^{-4}	111.2362
		Peak	19.0951×10^{-3}	31.7927×10^{-1}	49.7170×10^{-4}	878.6037
	Active: ASRE	RMS	2.2199×10^{-3}	3.4248×10^{-1}	4.6982×10^{-4}	113.1504
		Peak	19.0098×10^{-3}	31.1159×10^{-1}	49.8040×10^{-4}	898.7364
	Passive	RMS	4.5604×10^{-3}	8.5205×10^{-1}	10.3647×10^{-4}	
		Peak	36.5733×10^{-3}	84.1714×10^{-1}	112.2152×10^{-4}	
30	Active: SDRE	RMS	1.5412×10^{-3}	2.4739×10^{-1}	3.7627×10^{-4}	89.2376
		Peak	13.3394×10^{-3}	26.4232×10^{-1}	52.6483×10^{-4}	696.9390
	Active: ASRE	RMS	1.5409×10^{-3}	2.4622×10^{-1}	3.7624×10^{-4}	89.2218
		Peak	13.2983×10^{-3}	26.0875×10^{-1}	52.6826×10^{-4}	704.0930
	Passive	RMS	3.2718×10^{-3}	5.9854×10^{-1}	8.3991×10^{-4}	
		Peak	25.8389×10^{-3}	66.9599×10^{-1}	118.6790×10^{-4}	

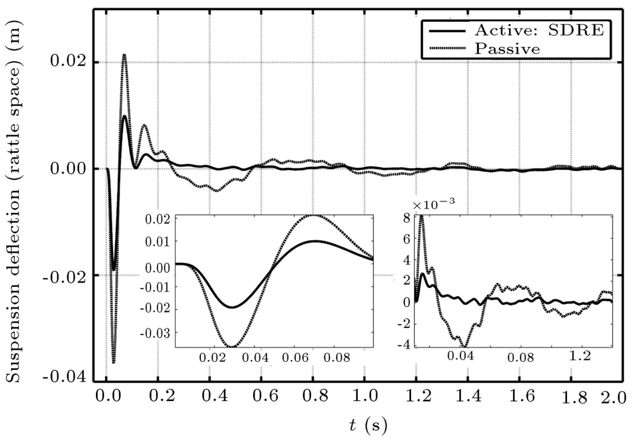

Figure 3. Difference between p_s and p_u.

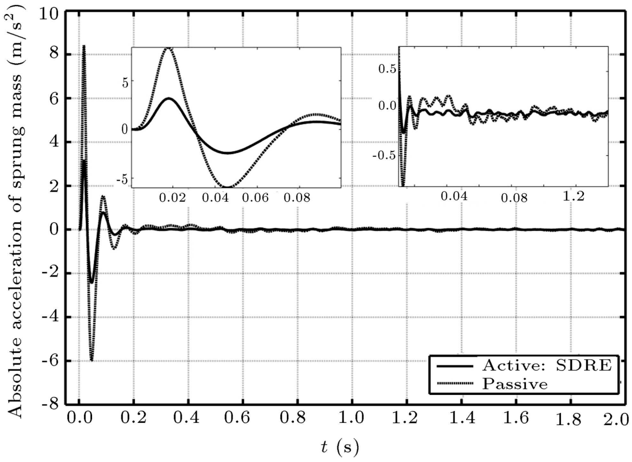

Figure 5. Second derivative of p_s.

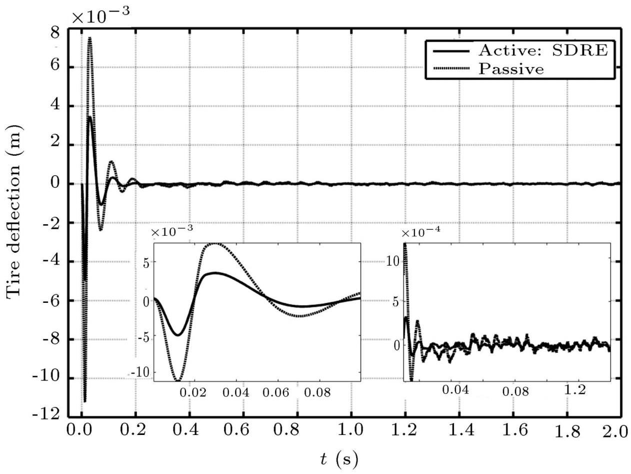

Figure 4. Difference between p_u and p_r.

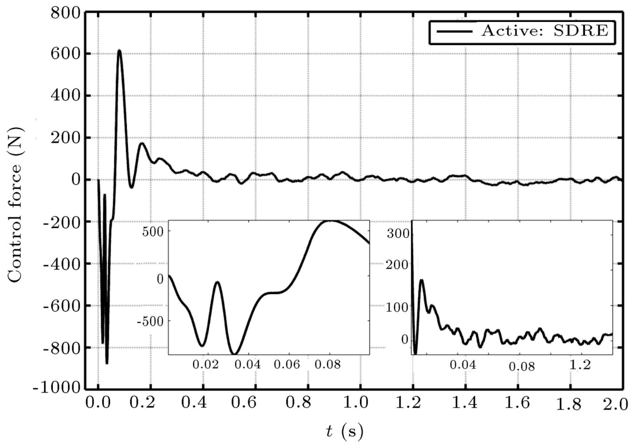

Figure 6. Control force.

In this section, the plots of the simulation results at the vehicle speed of 20 m/s are given. In this regard, first, the plots of the values of the variables obtained from the control method based on SDRE technique were given. They were then compared with the plots of the values of the variables of the equivalent PSS. Figure 3 shows the variation of the suspension deflection against time. Figure 4 presents the variation of the tire deflection against time. Figure 5 demonstrates the variation of the sprung mass acceleration against time. Figure 6 depicts the variation of the control force. Moreover, as a frequency domain analysis, the magnitudes of suspension deflection, tire deflection, and sprung mass acceleration against frequency are given in Figures 7, 8, and 9, respectively. In the frequency domain analysis, first, the power spectral densities for each variable were calculated. Then, the magnitudes of each variable were calculated through the common logarithm of the power spectral densities of each variable.

Second, the plots of the values of the variables obtained from the control method based on ASRE technique were presented. They were then compared

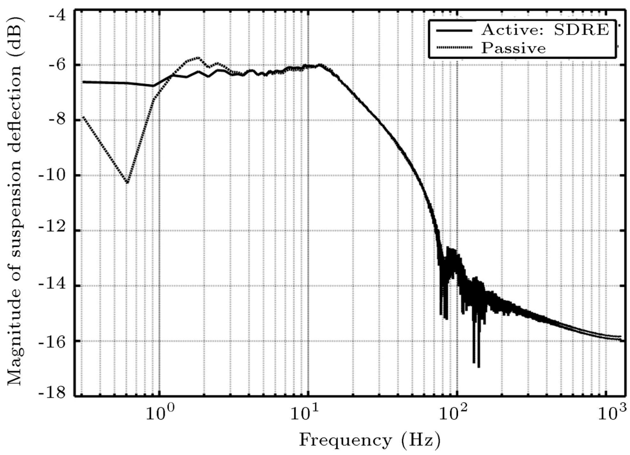

Figure 7. Magnitude of $p_s - p_u$.

with the values of the variables of the equivalent PSS. Figure 10 shows the variation of the suspension deflection against time. Figure 11 depicts the variation of the tire deflection against time. Figure 12 gives the variation of the sprung mass acceleration against time. Figure 13 presents the variation of the control

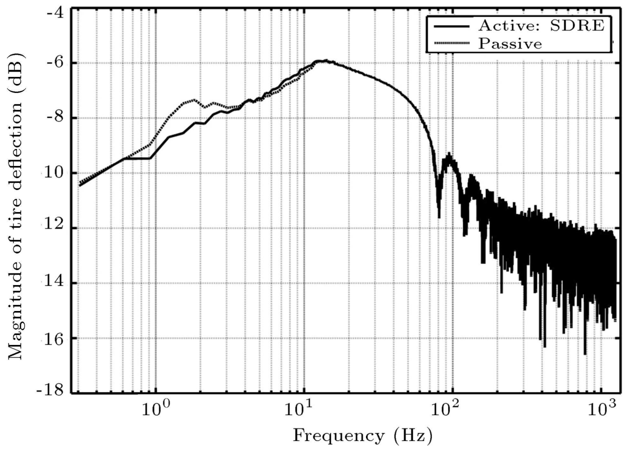

Figure 8. Magnitude of $p_u - p_r$.

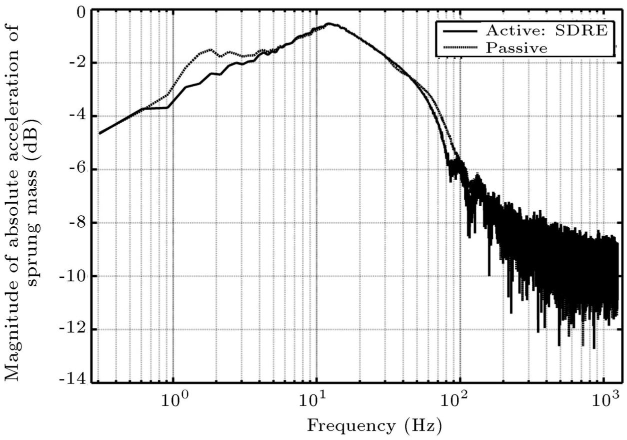

Figure 9. Magnitude of second derivative of p_s.

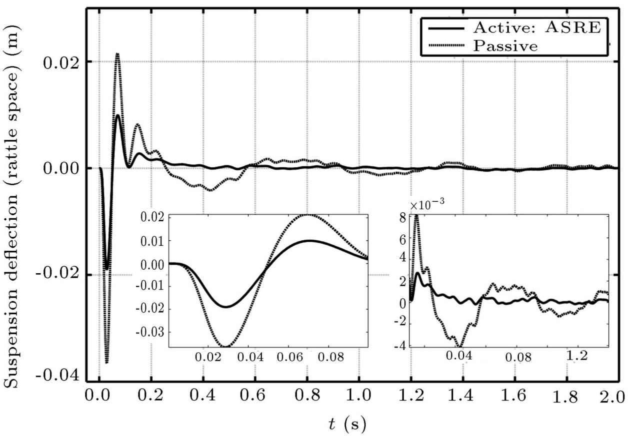

Figure 10. Difference between p_s and p_u.

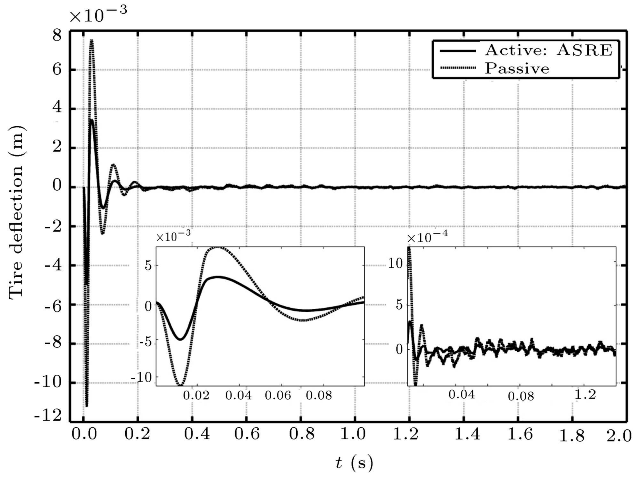

Figure 11. Difference between p_u and p_r.

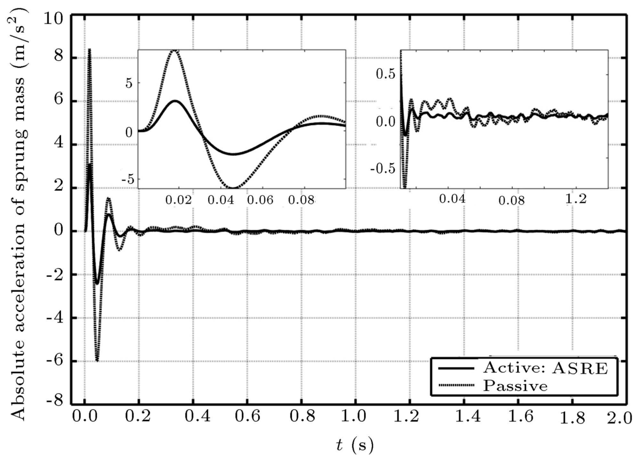

Figure 12. Second derivative of p_s.

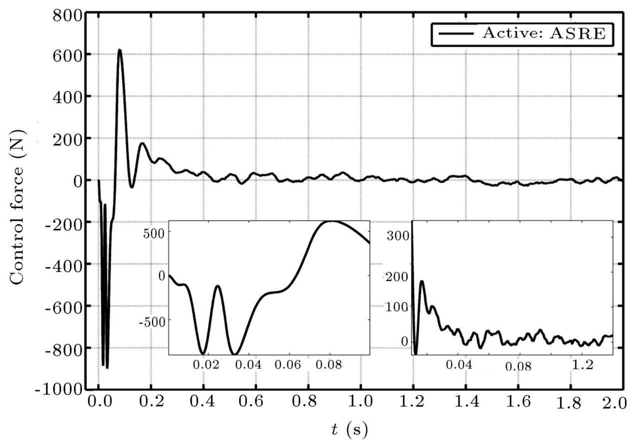

Figure 13. Control force.

force. Moreover, as a frequency domain analysis, the magnitudes of suspension deflection, tire deflection, and sprung mass acceleration against frequency are given in Figures 14, 15, and 16, respectively.

The case studies revealed that application of the developed control methods based on SDRE and ASRE techniques would result in satisfactory performance of the ASS. Of note, the simulation results of both control methods were close to each other. Simulations based on the developed control methods were checked against the performance requirements. They were also compared with those of the corresponding PSS. Followed by crossing the sinusoidal hump, oscillation

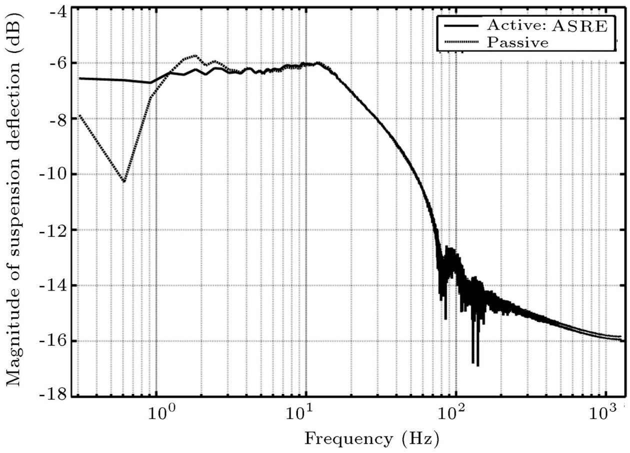

Figure 14. Magnitude of $p_s - p_u$.

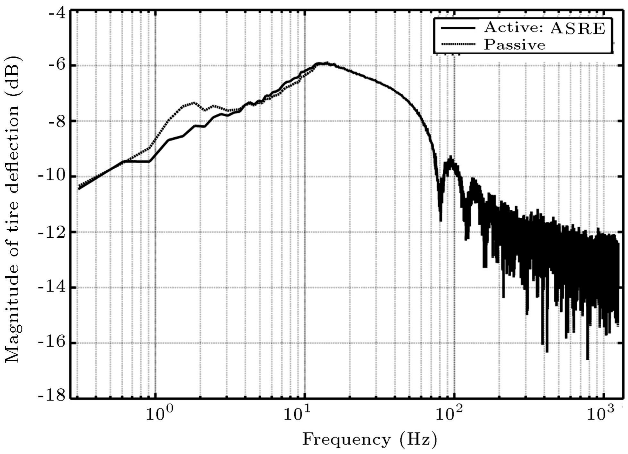

Figure 15. Magnitude of $p_u - p_r$.

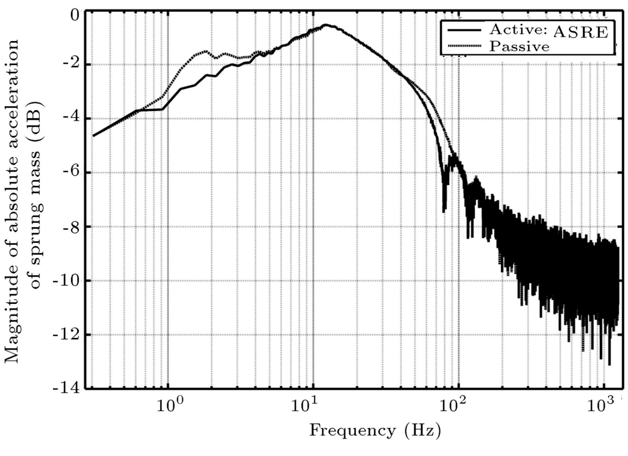

Figure 16. Magnitude of second derivative of p_s.

of the suspension and tire deflections of ASS were suppressed. As a result, as observed in Figures 3, 4 and 10, 11, they returned to their equilibrium positions in a very short time using both techniques when compared to the equivalent passive system. After settling down the ASS to its equilibrium state by means of control, the suspension deflection steady-state value were below 1.5×10^{-3} m and the tire deflection steady-state values were below 1.2×10^{-3} m. The maximum acceleration values of the sprung mass and control force were obtained, while the vehicle crossed the sinusoidal hump. The maximum acceleration values of the sprung mass and control force were calculated as 3 m/s^2 and 900 N, respectively.

As a two-DOF system, quarter vehicle SS has two undamped natural frequencies. In the case of an LTI quarter vehicle SS, when the suspension spring constant is much less than the tire spring constant, the undamped natural frequencies are approximated as $\omega_{n1} = \sqrt{k_s/m_s}$ and $\omega_{n2} = \sqrt{k_t/m_u}$. Here, ω_{n1} is less than ω_{n2}, each referring to the undamped natural frequencies of sprung and unsprung masses, respectively [44]. In the case of the quarter vehicle SS with nonlinear spring and damper used in this study, the two undamped natural frequencies were observed in the simulations of the PSS frequency domain analysis given in Figures 7–9 and 14–16.

If the equation of an SS vibration problem is independent of the passive and active suspension forces, it is called as invariant equation. Invariant points refer to the frequencies where ASS transfer function is the same as PSS transfer function irrespective of the actuator forces of ASS. For an LTI quarter vehicle SS, if the suspension spring constant is much less than tire spring constant, the sprung mass acceleration transfer function has an invariant point when the frequency is equal to the unsprung mass natural frequency $\omega_{inv1} = \sqrt{k_t/m_u}$, and the suspension deflection transfer function has an invariant point when the frequency is equal to $\omega_{inv2} = \sqrt{k_t/(m_s + m_u)}$ [44]. For the nonlinear quarter vehicle SS used in this study, the corresponding invariant points can be seen in Figures 9 and 16, and Figures 7 and 14.

Detectability of the system is satisfied by using a positive definite $\mathbf{Q}$. Stabilizability of the system is guaranteed by inspecting the controllability matrix at each step.

6. Conclusions

In this work, two methods, which were computationally simple and easily applicable, were developed based on SDRE and ASRE approaches to control ASS in the presence of nonlinear spring and damper. In addition, the effectiveness of these control methods was evaluated and compared with each other.

The nonlinear dynamics of the vehicle SS was expressed as the first-order differential equations in terms of conveniently selected state variables for better control performance. Additionally, a convenient representation of a cost function in terms of state variables was obtained to realize better control.

In both of the control methods, nonlinear dynamics was expressed in the form of an SDC and it was a linear like structure. Different SDC forms and weighting constants might be considered as design flexibility. It is implied that they may be used to improve the performances of the control techniques. Because the nonlinear equations are represented by linear equations, the linear controllers can be used in both of the methods.

In SDRE method, a nonlinear two-point boundary value problem is not needed to be solved; therefore, the technique is simple if the time for computation is taken into consideration. SDC structure should be selected such that $\{\mathbf{C}(\mathbf{y}), \mathbf{A}(\mathbf{y})\}$ must be pointwise detectable, while $\{\mathbf{A}(\mathbf{y}), \mathbf{B}(\mathbf{y})\}$ must be pointwise stabilizable.

In the case of ASRE method, the nonlinear system can be represented by using successive LTV equations. This technique can be used for systems having nonlinear dynamics that satisfy local Lipschitz requirement, which is very mild.

SDRE method determines the optimal feedback control online, while ASRE method determines the optimal feedback control to be offline since it uses an iteration procedure. Therefore, when the reference motion is not known in advance, SDRE method is ideal for real-time operations. Both of the methods give effective design schemes by only solving ARE and then, forming a nonlinear optimal control input. These schemes are obtained by extending linear quadratic optimal control method to nonlinear system. The methods are computationally simple and overcome many of the shortcomings and difficulties of linear quadratic optimal control method.

The case studies revealed that satisfactory performances were obtained for ASS using the developed control methods that utilized SDRE and ASRE techniques. Moreover, simulation results of both control methods were close to each other. Simulations obtained from the developed control methods were checked against the performance requirements, and they were compared with the simulation of corresponding PSS to illustrate the effectiveness of the both control methods. Performance requirements were fulfilled by using both control methods. After crossing the sinusoidal hump, oscillation of ASS sprung mass was suppressed and it came back to its equilibrium position in a very short time by using both techniques when compared to the equivalent passive system. The maximum values of the acceleration of the sprung mass and control force were monitored while the vehicle passing the sinusoidal bump.

Nomenclature

a	Constant
$\mathbf{A}(\mathbf{y})$	SDC matrix
ASRE	Approximating Sequence of Riccati Equation
ASS	Active Suspension System
$\mathbf{B}(\mathbf{y})$	SDC matrix
b_s, b_{ns}	Nonlinear damper constants
D	Hump width
DOF	Degree Of Freedom
$\mathbf{f}(\mathbf{y})$	Nonlinear function
$\mathbf{F}(\mathbf{y}(t_f))$	Endpoint matrix
F_a	Magnitude of the driving force
h	Hump height
$\mathbf{J}$	Cost function
LTI	Linear Time Invariant
LTV	Linear Time Varying
m_s	Mass of the vehicle body (sprung mass)
m_u	Masses of the tire and axles (unsprung mass)
k_s, k_{ns}	Nonlinear spring constants
k_t	Spring coefficient of the stiffness of the tire
p_r	Road disturbance at position level
p_s	Position of the sprung mass
p_u	Position of the unsprung mass
$\mathbf{P}(\mathbf{y})$	Control weighting matrix
PSD	Power Spectral Density
PSS	Passive Suspension System
$\mathbf{Q}(\mathbf{y})$	State weighting matrix
RMS	Root-Mean-Square
SDC	State Dependent Coefficient
SDRE	State Dependent Riccati Equation
SS	Suspension System
t_0	Time where the hump starts
t_r	Time where the hump finishes
$\mathbf{u}(t)$	Vector of inputs
v	Speed of the vehicle
$w(t)$	Gaussian white noise process
$\mathbf{y}(t)$	Vector of states
y_1	Suspension deflection (rattle space)
y_2	Sprung mass absolute velocity
y_3	Tire deflection
y_4	Unsprung mass absolute velocity
γ	Constant
λ	Dummy variable for integration
$\lambda_i(\cdot)$	Eigenvalues of a matrix
σ^2	Variance of road roughness

$\mathbf{\Phi}^{[k-1]}(t,t_0)$	Transition matrix of $\mathbf{A}(\mathbf{y}^{[k-1]}(t))$
$\psi(\omega)$	PSD function
ω	Circular frequency
ω_{inv1}	Sprung mass acceleration transfer function invariant point frequency
ω_{inv2}	Suspension deflection transfer function invariant frequency
ω_{n1}	Sprung mass undamped natural frequency
ω_{n2}	Unsprung mass undamped natural frequency

References

1. Marzbanrad, J., Hojjat, Y., Zohoor, H., et al. "Optimal preview control design of an active suspension based on a full car model", *Scientia Iranica*, **10**(1), pp. 23–36 (2003).
2. Sayyaadi, H. and Shokouhi, N. "New dynamics model for rail vehicles and optimizing air suspension parameters using GA", *Scientia Iranica B*, **16**(6), pp. 496–512 (2009).
3. Soleymani, M., Montazeri-Gh, M., and Amiryan, R. "Adaptive fuzzy controller for vehicle active suspension system based on traffic conditions", *Scientia Iranica B*, **19**(3), pp. 443–453 (2012).
4. Fakhraei, J., Khanlo, H.M., and Ghayour, M. "Chaotic behaviors of a ground vehicle oscillating system with passengers", *Scientia Iranica B*, **24**(3), pp. 1051–1068 (2017).
5. Dumitriu, M. "Numerical study of the influence of suspended equipment on ride comfort in high-speed railway vehicles", *Scientia Iranica B*, **27**(4), pp. 1897–1915 (2020).
6. Rezazadeh, A. and Moradi, H. "Design of optimum vibration absorbers for a bus vehicle to suppress unwanted vibrations against harmonic and random road excitations", *Scientia Iranica B*, **28**(1), pp. 241–254 (2021).
7. Malekshahi, A., Mirzaei, M., and Aghasizade, S. "Nonlinear predictive control of multi-input multi-output vehicle suspension system", *Journal of Low Frequency Noise, Vibration and Active Control*, **34**(1), pp. 87–106 (2015).
8. Liang, Y.-J., Li, N., Gao, D.-X., et al. "Optimal vibration control for nonlinear systems of tracked vehicle half-car suspensions", *International Journal of Control, Automation and Systems*, **15**(4), pp. 1675–1683 (2017).
9. Abdalla, M.O., Al Shabatat, N., and Al Qaisi, M. "Linear matrix inequality based control of vehicle active suspension system", *Vehicle System Dynamics*, **47**(1), pp. 121–134 (2009).
10. Pusadkar, U.S., Chaudhari, S.D., Shendge, P.D., et al. "Linear disturbance observer based sliding mode control for active suspension systems with non-ideal actuator", *Journal of Sound and Vibration*, **442**, pp. 428–444 (2019).
11. Deshpande, V.S., Mohan, B., Shendge, P.D., et al. "Disturbance observer based sliding mode control of active suspension systems", *Journal of Sound and Vibration*, **333**, pp. 2281–2296 (2014).
12. Wang, D., Zhao, D., Gong, M., et al. "Nonlinear predictive sliding mode control for active suspension system", *Shock and Vibration*, **2018**, pp. 1–10 (2018).
13. Rath, J.J., Veluvolu, K.C., and Defoort, M. "Active control of nonlinear suspension system using modified adaptive supertwisting controller", *Discrete Dynamics in Nature and Society*, **2015**, pp. 1–10 (2015).
14. Wang, H., Lu, Y., Tian, Y., et al. "Fuzzy sliding mode based active disturbance rejection control for active suspension system", *Proc. IMechE. Part D: J. Automobile Engineering*, **234**(2-3), pp. 449–457 (2020).
15. Rui, B "Nonlinear adaptive sliding-mode control of the electronically controlled air suspension system", *International Journal of Advanced Robotic Systems*, **16**(5), pp. 1–6 (2019).
16. Zhang, Y., Liu, Y., and Liu, L. "Minimal learning parameters-based adaptive neural control for vehicle active suspensions with input saturation", *Neurocomputing*, **396**, pp. 153–161 (2020).
17. Huang, Y., Na, J., Wu, X., et al. "Adaptive control of nonlinear uncertain active suspension systems with prescribed performance", *ISA Transactions*, **54**, pp. 145–155 (2015).
18. Zhu, Y. and Zhu, S. "Nonlinear time-delay suspension adaptive neural network active control", *Abstract and Applied Analysis*, **2014**, pp. 1–6 (2014).
19. Pan, H., Sun, W., Jing, X., et al. "Adaptive tracking control for active suspension systems with non-ideal actuators", *Journal of Sound and Vibration*, **399**, pp. 2–20 (2017).
20. Pang, H., Zhang, X., and Xu, Z. "Adaptive backstepping-based tracking control design for nonlinear active suspension system with parameter uncertainties and safety constraints", *ISA Transactions*, **88**, pp. 23–36 (2019).
21. Na, J., Huang, Y., Wu, X., et al. "Active adaptive estimation and control for vehicle active suspensions with prescribed performance", *IEEE Transactions on Control Systems Technology*, **26**(6), pp. 2063–2077 (2018).
22. Yao, J., Zhang, J.Q., Zhao, M.M., et al. "Active control of a nonlinear suspension with output constraints and variable-adaptive-law control", *Journal of Vibroengineering*, **20**(7), pp. 2690–2704 (2018).
23. Yao, J., Zhang, J.Q., Zhao, M.M., et al. "Adaptive control of a nonlinear suspension with time delay compensation", *Journal of Vibroengineering*, **21**(3), pp. 684–695 (2019).

24. Qin, W., Ge, P., Liu, F., et al. "Adaptive robust control for active suspension systems: targeting nonholonomic reference trajectory and large mismatched uncertainty", *Nonlinear Dyn.*, **104**, pp. 3861–3880 (2021).

25. Qin, W., Liu, F., Yin, H., et al. "Constraint-based adaptive robust control for active suspension systems under sky-hook model", *IEEE Transactions on Industrial Electronics*, **69**(5), pp. 5152–5164 (2022).

26. Pan, H., Sun, W., Gao, H., et al. "Constrained robust adaptive control for vehicle active suspension systems", *Int. J. Vehicle Design*, **68**(1/2/3), pp. 5–21 (2015).

27. Zhang, J., Ding, F., Zhang, B., et al. "An effective projection-based nonlinear adaptive control strategy for heavy vehicle suspension with hysteretic leaf spring", *Nonlinear Dyn.*, **100**, pp. 451–473 (2020).

28. Ding, F., Li, Q., Jiang, C., et al. "Event-triggered control for nonlinear leaf spring hydraulic actuator suspension system with valve predictive management", *Information Sciences*, **551**, pp. 184–204 (2021).

29. Wu, Y., Li, B., Du, H., et al. "Fault-tolerant prescribed performance control of active suspension based on approximation-free method", *Vehicle System Dynamics*, **60**(5), pp. 1642-1667 (2022).

30. Lu, Y., Wang, H., and Tian, Y. "Active disturbance rejection control for active suspension system of nonlinear full car", *2018 IEEE 7th Data Driven Control and Learning Systems Conference*, Enshi, Hubei Province, China, pp. 724–729 (2018).

31. Nourisola, H. and Ahmadi, B. "Robust adaptive Hinfinity controller based on GA-Wavelet-SVM for nonlinear vehicle suspension with time delay actuator", *Journal of Vibration and Control*, **22**(20), pp. 4111–4120 (2016).

32. Zhang, M. and Jing, X. "Switching logic-based saturated tracking control for active suspension systems based on disturbance observer and bioinspired X-dynamics", *Mechanical Systems and Signal Processing*, **155**, p. 107611 (18 pages) (2021).

33. Demir, O., Keskin, I., and Cetin, S. "Modeling and control of a nonlinear half-vehicle suspension system: A hybrid fuzzy logic approach", *Nonlinear Dyn.*, **67**(3), pp. 2139–2151 (2012).

34. Aldair, A.A. and Wang, W.J. "A neurofuzzy controller for full vehicle active suspension systems", *Journal of Vibration and Control*, **18**(12), pp. 1837–1854 (2011).

35. Cimen, T. "Systematic and effective design of nonlinear feedback controllers via the state-dependent Riccati equation (SDRE) method", *Annual Reviews in Control*, **34**(1), pp. 32–51 (2010).

36. Kilicaslan, S. "Tracking control of elastic joint parallel robots via state-dependent Riccati equation", *Turk J. Elec. Eng. & Comp. Sci.*, **23**(2), pp. 522–538 (2015).

37. Banks, S.P. and Dinesh, K. "Approximate optimal control and stability of nonlinear finite and infinite-dimensional systems", *Annals of Operations Research*, **98**(1–4), pp. 19–44 (2000).

38. Kilicaslan, S. and Banks, S.P. "A separation theorem for nonlinear systems", *Automatica*, **45**(4), pp. 928–935 (2009).

39. Kilicaslan, S. and Banks, S.P. "Existence of solutions of Riccati differential equations", *ASME Journal of Dynamic Systems, Measurement, and Control*, **134**(3), p. 031001 (11 pages) (2012).

40. Beltran-Carbajal, F., Chavez-Conde, E., Favela-Contreras, A., et al. "Active nonlinear vehicle suspension based on real time estimation of perturbation signals", *Proceedings of the 2011 IEEE International Conference on Industrial Technology (ICIT)*, Auburn, AL, USA, pp. 437–442 (2011).

41. Giua, A., Melas, M., Seatzu, C., et al. "Design of a predictive semiactive suspension system", *Vehicle System Dynamics*, **41**(4), pp. 277–300 (2004).

42. Pedro, J.O., Dangor, M., Dahunsi, O.A., et al. "Intelligent feedback linearization control of nonlinear electrohydraulic suspension systems using particle swarm optimization", *Applied Soft Computing*, **24**, pp. 50–62 (November 2014).

43. ISO 2631 "Mechanical vibration and shock-evaluation of human exposure to whole-body vibration-Part 1: General requirements", International Organization for Standardization, Geneva, Switzerland (2003).

44. Rajamani, R. "Active automotive suspensions", In *Vehicle Dynamics and Control*, pp. 341–347, Springer, NY, USA (2006).

Biography

Sinan Kilicaslan is an Associate Professor of Mechanical Engineering at Gazi University, Ankara, Turkey. He received the PhD in Mechanical Engineering from the Middle East Technical University, Ankara, Turkey. His research interests include dynamics and control of rigid and flexible mechanical systems and nonlinear, optimal, deterministic, and stochastic estimation and control theory.